Crystal structure of 4-bromo-5,7-dimethoxy-2,3-dihydro-1H-inden-1-one

Sri Hari Galla,[a] Jayalakshmi Sridhar,[a]* Joel T. Mague,[b] Xiaodong Zhang,[b] Kira D. White,[a] Qiang Zhang[a] and James P. Donahue[b]*

[a]Department of Chemistry, Xavier University of Louisiana, 1 Drexel Dr., New Orleans, Louisiana 70125, USA, and [b]Department of Chemistry, Tulane University, 6400 Freret Street, New Orleans, Louisiana 70118-5698, USA. *Correspondence e-mail: jsridhar@xula.edu, donahue@tulane.edu
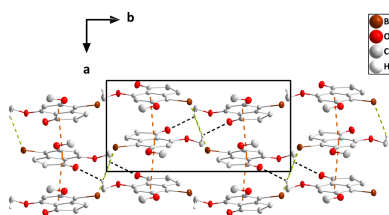
In the title molecule, $C_{11}H_{11}BrO_3$, the dihydroindene moiety is essentially planar but with a slight twist in the saturated portion of the five-membered ring. The methoxy groups lie close to the above plane. In the crystal, π-stacking interactions between six-membered rings form stacks of molecules extending along the a-axis direction, which are linked by weak C—H⋯O and C—H⋯Br hydrogen bonds. A Hirshfeld surface analysis was performed showing H⋯H, O⋯H/H⋯O and Br⋯H/H⋯Br contacts make the largest contributions to intermolecular interactions in the crystal.

1. Chemical context

Aberrant expression of protein kinases is a hallmark of several cancers, and small molecules targeting specific kinases are in clinical use as cancer therapeutics (Du & Lovly, 2018; Kannaiyan & Mahadevan, 2018; Roskoski, 2023). Development of resistance to the kinase inhibitors is a frequent occurrence, which motivates a continuing search for new kinase inhibitors (Yang et al., 2022). One of the key characteristics of the kinase inhibitors is the capacity to form two hydrogen bonds, one as donor and one as acceptor, with the hinge region of the kinase (Arter et al., 2022; Attwood et al., 2021). Planarity with two functional groups capable of making the two essential hydrogen bonds, along with other substituents to target the unique residues of the ATP binding pocket for potency and specificity, are the fundamental structural features of kinase inhibitors.

We have developed 5-hydroxy-1,4-naphthoquinones as HER2 and PIM1 kinase inhibitors (Schroeder et al., 2014, 2016; Sridhar et al., 2014). To circumvent the issue of oxidation-reduction reactions of the quinone moiety, 5,7-dihydroxy-2,3-dihydro-1H-inden-1-one is currently under development as a new core structure. The new series based upon this platform is capable of making the requisite hydrogen bonds to the kinase hinge region and has potential for functionalization at the 2, 3, 4, 5 and 6 positions to enable specific and potent inhibition of the kinase of interest. Bromination serves as an initial step for functionalizing the core structure of 5,7-dimethoxy-2,3-dihydro-1H-inden-1-one.

Bromination by free radical or electrophilic aromatic substitution mechanisms using N-bromosuccinimide (NBS) is known to introduce a bromine atom on an allylic or benzylic carbon atom or on an aromatic ring (Djerassi, 1948; Li et al., 2014). When subjected to bromination with NBS in benzene in the presence of azobisisobutyronitrile (AIBN) for 15 h at ambient temperature, 5,7-dimethoxy-2,3-dihydro-1H-inden-1-
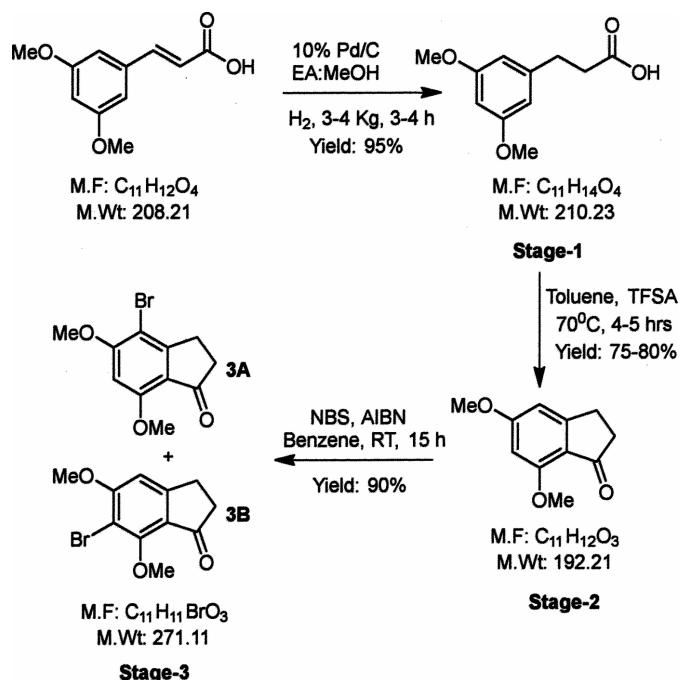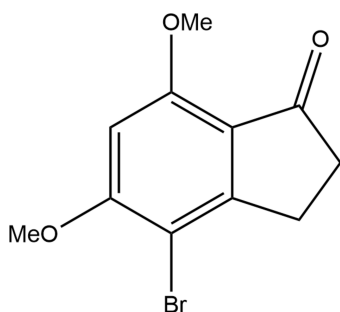
Figure 1
Synthesis scheme for 4-bromo-5,7-dimethoxy-2,3-dihydro-1*H*-inden-1-one.

Figure 2
The title molecule with labeling scheme and 50% probability displacement ellipsoids.

3. Supramolecular features

In the crystal (Fig. 3), the molecules stack along the *a*-axis direction with significant π interactions between the C1–C6 rings [centroid–centroid distance = 3.5606 (16) Å, dihedral angle = 1.61 (13)°, slippage alternates between 0.93 and

one yielded a single product. From among the product outcomes depicted as **1A**, **1B** and **1C** in Fig. 1, NMR spectroscopy indicated that electrophilic aromatic substitution had occurred to form a single species – either **1A** or **1B**. X-ray crystallography has identified the product as **1B** (Fig. 2), the detailed structural characterization and crystal packing arrangement of which we describe herein.

Figure 3
A portion of one stack viewed along the *c*-axis direction with the π-stacking interactions depicted by dashed lines. Non-interacting hydrogen atoms are omitted for clarity.

2. Structural commentary

The dihydroindene moiety is planar to within 0.045 (3) Å (r.m.s. deviation of the contributing atoms = 0.003 Å) with C9 that distance from one side of the mean plane and C8 0.018 (4) Å from the opposite side. This twist in the five-membered ring is towards the upper end of the range seen in related structures (see *Database survey*). Both methoxy groups are nearly coplanar with the C1–C6 ring as indicated by the C10—O1—C3—C4 and C11—O2—C5—C4 torsion angles which are, respectively, 2.7 (4) and 6.6 (5)°. All bond distances and interbond angles are as expected for the formulation given.
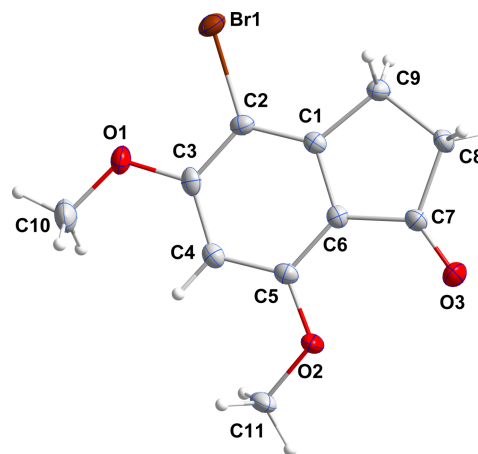

Figure 4
Packing viewed along the *c*-axis direction with the C—H⋯O and C—H⋯Br hydrogen bonds depicted, respectively, by black and green dashed lines. The π-stacking interactions are depicted by orange dashed lines and non-interacting hydrogen atoms are omitted for clarity.

Table 1
Hydrogen-bond geometry (Å, °).

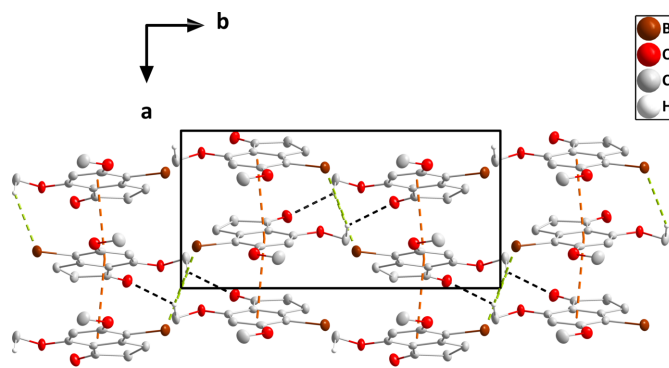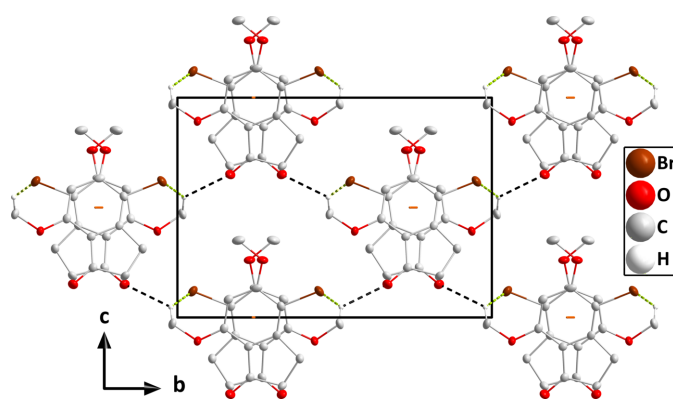| D—H$\cdots A$	D—H	H$\cdots A$	$D\cdots A$	D—H$\cdots A$
C11—H11$A\cdots$Br1^i	0.98	3.06	3.605 (4)	116
C11—H11$C\cdots$Br1^{ii}	0.98	2.90	3.683 (3)	137
C11—H11$C\cdots$O3^{iii}	0.98	2.58	3.288 (4)	129

Symmetry codes: (i) $-x+\frac{1}{2}, y-\frac{1}{2}, z-\frac{1}{2}$; (ii) $x+\frac{1}{2}, -y+\frac{3}{2}, z$; (iii) $-x+1, -y+1, z+\frac{1}{2}$.
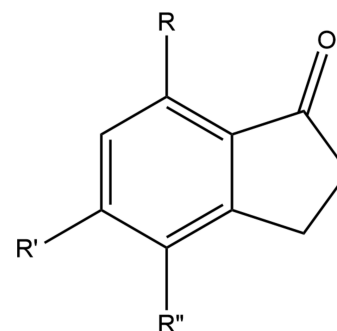
0.96 Å]. The stacks are linked by weak C11—H11$C\cdots$O3 and C11—H11$C\cdots$Br1 hydrogen bonds (Table 1 and Figs. 4 and 5).

4. Database survey

A search of the Cambridge Structural Database (CSD; updated to May 2024; Groom *et al.*, 2016) with the search fragment shown in Fig. 6 returned 58 hits of which 25 are most similar to the title molecule with the remainder having additional rings fused to the aromatic ring or being metal complexes. Interestingly, there are no examples with three substituents on the six-membered ring, but the search found 18 structures with one substituent, six with two and the unsubstituted parent molecule ($R = R' = R'' = $ H, QQQGMJ; Morin *et al.*, 1974, QQQGMJ01; Peña Ruiz *et al.*, 2004). There are two structures with $R'' = $ Br, namely AWOBOF ($R = R' = $ H; Aldeborgh *et al.*, 2014) and LAQCAJ ($R = $ H, $R' = $ NH$_2$; Çelik *et al.*, 2012), and one with $R = R' = $ OMe, $R'' = $ H (MXINDO10; Gupta *et al.*, 1984). The other structures with two substituents have $R = $ OMe, $R' = $ H, $R'' = $ 4-fluorobenzoyl (CAPHEJ; Chang & Lee, 2011), $R = $ OH, $R' = $ H, $R'' = $ 4-methoxybenzoyl (CAPHIN; Chang & Lee, 2011), $R = $ H, $R' = $ H, $R'' = $ OPr^i (CETCAG; Coyanis *et al.*, 2006) and $R' = $ H, $R = R'' = $ Me (MUQCEG; Johnson *et al.*, 2002). In AWOBOF and LAQCAJ, the C—Br distances are virtually the same as in the title molecule [1.892 (3) Å] and the twist in the five-membered ring is slightly less. Among the other disubstituted molecules, the greatest deviation of the saturated carbon atoms of the five-membered ring from the mean plane of the bicyclic moiety is in CAPHIN [0.091 (2) and −0.122 (2) Å] while the least is in MUQCEG [0.016 (3) and

Figure 6
The fragment used in the database survey.

−0.012 (3) Å]. As in the title molecule, the methyl carbon atoms of the methoxy groups in CAPHEJ, CETCAG and MXINDO10 lie in or very close to the mean plane of the nine-membered ring system. Where π-stacking of the six-membered aromatic rings occurs in the disubstituted examples, this involves only pairs of molecules (LAQCAJ and MXINDO10) rather than extended stacks.

5. Hirshfeld surface analysis

The Hirshfeld surface was constructed with *CrystalExplorer 21.5* (Spackman *et al.*, 2021) with descriptions of the several

(a)

(b)

Figure 7
The Hirshfeld surface plotted over (*a*) d_{norm} and (*b*) over the shape index including two additional molecules in the stack plus two more in an adjacent stack with the C—H$\cdots$O and C—H$\cdots$Br hydrogen bonds shown by green dashed lines.

Figure 5
Packing viewed along the *a*-axis direction with the C—H$\cdots$O and C—H$\cdots$Br hydrogen bonds depicted, respectively, by black and green dashed lines. The π-stacking interactions are depicted by orange dashed lines and non-interacting hydrogen atoms are omitted for clarity.
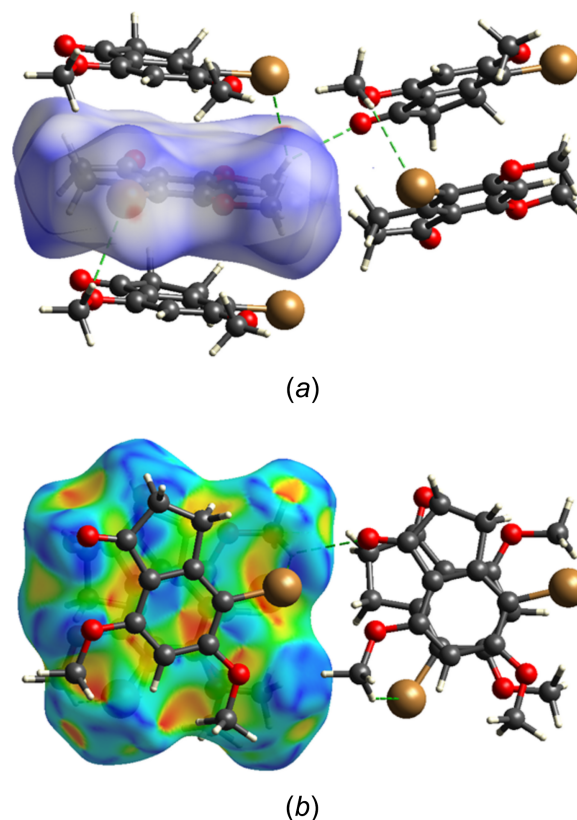
(a)

(b)

(c)

(d)

(e)

Figure 8
Fingerprint plots showing (*a*) all contacts, (*b*) H···H contacts, (*c*) O···H/ H···O contacts, (*d*) Br···H/H···Br contacts, and (*e*) C···C contacts.

Table 2
Experimental details.

Crystal data	
Chemical formula	$C_{11}H_{11}BrO_3$
M_r	271.11
Crystal system, space group	Orthorhombic, $Pna2_1$
Temperature (K)	150
a, b, c (Å)	7.0928 (5), 14.3933 (10), 10.0419 (7)
V (Å^3)	1025.17 (12)
Z	4
Radiation type	Mo $K\alpha$
μ (mm^{-1})	3.99
Crystal size (mm)	$0.22 \times 0.06 \times 0.03$
Data collection	
Diffractometer	Bruker D8 QUEST PHOTON 3 diffractometer
Absorption correction	Numerical (*SADABS*; Krause *et al.*, 2015)
T_{min}, T_{max}	0.70, 0.89
No. of measured, independent and observed [$I > 2\sigma(I)$] reflections	13923, 2534, 2366
R_{int}	0.030
$(\sin\theta/\lambda)_{max}$ (Å^{-1})	0.667
Refinement	
$R[F^2 > 2\sigma(F^2)], wR(F^2), S$	0.025, 0.056, 1.08
No. of reflections	2534
No. of parameters	139
No. of restraints	1
H-atom treatment	H-atom parameters constrained
$\Delta\rho_{max}, \Delta\rho_{min}$ (e Å^{-3})	0.41, −0.39
Absolute structure	Flack x determined using 1025 quotients [$(I^+)-(I^-)$]/[$(I^+)+(I^-)$] (Parsons *et al.*, 2013). Refined as an inversion twin
Absolute structure parameter	0.039 (12)

Computer programs: *APEX4* and *SAINT* (Bruker, 2021), *SHELXT/5* (Sheldrick, 2015*a*), *SHELXL2019/1* (Lübben *et al.*, 2019; Sheldrick, 2015*b*), *DIAMOND* (Brandenburg & Putz, 2012) and *SHELXTL* (Sheldrick, 2008).

6. Synthesis and crystallization

To a solution of 5,7-dimethoxy-2,3-dihydro-1*H*-inden-1-one (1.0 g, 5.2 mmol) in benzene (15 mL) were added *N*-bromo-succinimide (0.93 g, 5.2 mmol) and a catalytic amount of azobisisobutyronitrile at room temperature. This reaction mixture was stirred for 15 h, with progress being monitored by TLC. Upon completion of the reaction, the benzene was removed by distillation, and water was added. The resulting slurry was stirred for 30 min, and the crude 4-bromo-5,7-dimethoxy-2,3-dihydro-1*H*-inden-1-one was then collected by vacuum filtration and dried on the filter by continued application of the vacuum for an additional 30 min. Yield: 1.27 g of off-white solid, 4.7 mmol, 90%, m.p. 498–500 K. R_f: 0.4 (1:1 ethyl acetate:hexane). ^{1}H NMR (δ, ppm in DMSO-d_6): 6.64 (*s*, 1 H), 3.97 (*s*, 3 H), 3.88 (*s*, 3 H), 2.87–2.84 (*m*, 2 H), 2.55–2.52 (*m*, 2 H). ^{13}C NMR (δ, ppm in DMSO-d_6): 201.62, 162.29, 158.85, 157.96, 120.11, 99.75, 96.44, 57.66, 56.55, 37.01, 27.31. HRMS [$M + H$]$^+$: ^{79}Br calculated, 270.9970; found, 270.9974; ^{81}Br calculated, 272.9949; found, 272.9946. The NMR spectra (see supporting information) were acquired using a Bruker 400 MHz spectrometer, while the mass spectrum was obtained using a Thermo LTQ-Orbitrap LC/MS/MS System/UltiMate 3000 HPLC. The compound was crystallized from 15% ethyl acetate in hexane.

plots obtained and their interpretations described elsewhere (Tan *et al.*, 2019). Fig. 7*a* shows the surface plotted over d_{norm} in the range −0.1265 to 1.2968 in arbitrary units with four neighboring molecules. The two above and below the surface constitute part of the column formed by the π-stacking interactions, while the two at the right are part of an adjacent column showing the C—H···O and C—H···Br hydrogen bonds that link columns. Fig. 7*b* shows the surface plotted over the shape function and the flat area in the center containing red and blue triangles clearly shows the π-stacking interactions. The 2-D fingerprint plots are shown in Fig. 8, from which it was determined that H···H contacts contribute 37.1% of the total (Fig. 8*b*) while O···H/H···O (Fig. 8*c*) and Br···H/H···Br (Fig. 8*d*) contacts contribute, respectively, 26.3% and 16.8%. The C···C contacts, which are primarily the π-stacking interactions, contribute 9.8%. Other contacts make minimal contributions.

7. Refinement

Crystal data, data collection and structure refinement details are summarized in Table 2. Hydrogen atoms were included as riding contributions in idealized positions with isotropic displacement parameters tied to those of the attached atoms. One reflection affected by the beamstop was omitted from the final refinement.

Acknowledgements

Funding information

References

Aldeborgh, H., George, K., Howe, M., Lowman, H., Moustakas, H., Strunsky, N. & Tanski, J. M. (2014). *J. Chem. Crystallogr.* **44**, 70–81.

Arter, C., Trask, L., Ward, S., Yeoh, S. & Bayliss, R. (2022). *J. Biol. Chem.* **298**, 102247.

Attwood, M. M., Fabbro, D., Sokolov, A. V., Knapp, S. & Schiöth, H. B. (2021). *Nat. Rev. Drug Discov.* **20**, 839–861.

Brandenburg, K. & Putz, H. (2012). *DIAMOND*. Crystal Impact GbR, Bonn, Germany.

Bruker (2021). *APEX4* and *SAINT*. Bruker AXS LLC, Madison, Wisconsin, USA.

Çelik, İ., Akkurt, M., Yılmaz, M., Tutar, A., Erenler, R. & García-Granda, S. (2012). *Acta Cryst.* E**68**, o833.

Chang, M.-Y. & Lee, N.-C. (2011). *J. Chin. Chem. Soc.* **58**, 306–308.

Coyanis, E. M., Panayides, J.-L., Fernandes, M. A., de Koning, C. B. & van Otterlo, W. A. L. (2006). *J. Organomet. Chem.* **691**, 5222–5239.

Djerassi, C. (1948). *Chem. Rev.* **43**, 271–317.

Du, Z. & Lovly, C. M. (2018). *Mol. Cancer*, **17**, 58.

Groom, C. R., Bruno, I. J., Lightfoot, M. P. & Ward, S. C. (2016). *Acta Cryst.* B**72**, 171–179.

Gupta, M. P., Lenstra, A. T. H. & Geise, H. J. (1984). *Acta Cryst.* C**40**, 1846–1848.

Johnson, B. A., Kleinman, M. H., Turro, N. J. & Garcia-Garibay, M. A. (2002). *J. Org. Chem.* **67**, 6944–6953.

Kannaiyan, R. & Mahadevan, D. (2018). *Expert Rev. Anticancer Ther.* **18**, 1249–1270.

Krause, L., Herbst-Irmer, R., Sheldrick, G. M. & Stalke, D. (2015). *J. Appl. Cryst.* **48**, 3–10.

Li, H.-J., Wu, Y.-C., Dai, J.-H., Song, Y., Cheng, R. & Qiao, Y. (2014). *Molecules* **19**, 3401–3416.

Lübben, J., Wandtke, C. M., Hübschle, C. B., Ruf, M., Sheldrick, G. M. & Dittrich, B. (2019). *Acta Cryst.* A**75**, 50–62.

Morin, Y., Brassy, C. & Mellier, A. (1974). *J. Mol. Struct.* **20**, 461–469.

Parsons, S., Flack, H. D. & Wagner, T. (2013). *Acta Cryst.* B**69**, 249–259.

Peña Ruiz, T., Fernández-Gómez, M., López González, J. J., Koziol, A. E. & Granadino Roldán, J. M. (2004). *J. Mol. Struct.* **707**, 33–46.

Roskoski, R. Jr (2023). *Pharmacol. Res.* **187**, 106552.

Schroeder, R. L., Goyal, N., Bratton, M., Townley, I., Pham, N. A., Tram, P., Stone, T., Geathers, J., Nguyen, K. & Sridhar, J. (2016). *Bioorg. Med. Chem. Lett.* **26**, 3187–3191.

Schroeder, R. L., Stevens, C. L. & Sridhar, J. (2014). *Molecules*, **19**, 15196–15212.

Sheldrick, G. M. (2008). *Acta Cryst.* A**64**, 112–122.

Sheldrick, G. M. (2015a). *Acta Cryst.* A**71**, 3–8.

Sheldrick, G. M. (2015b). *Acta Cryst.* C**71**, 3–8.

Spackman, P. R., Turner, M. J., McKinnon, J. J., Wolff, S. K., Grimwood, D. J., Jayatilaka, D. & Spackman, M. A. (2021). *J. Appl. Cryst.* **54**, 1006–1011.

Sridhar, J., Sfondouris, M. E., Bratton, M. R., Nguyen, T. L., Townley, I., Klein Stevens, C. L. & Jones, F. E. (2014). *Bioorg. Med. Chem. Lett.* **24**, 126–131.

Tan, S. L., Jotani, M. M. & Tiekink, E. R. T. (2019). *Acta Cryst.* E**75**, 308–318.

Yang, Y., Li, S., Wang, Y., Zhao, Y. & Li, Q. (2022). *Sig Transduct. Target. Ther.* **7**, 329.

Crystal structure of 4-bromo-5,7-dimethoxy-2,3-dihydro-1*H*-inden-1-one

Sri Hari Galla, Jayalakshmi Sridhar, Joel T. Mague, Xiaodong Zhang, Kira D. White, Qiang Zhang and James P. Donahue

Computing details

4-Bromo-5,7-dimethoxy-2,3-dihydro-1*H*-inden-1-one

Crystal data

$C_{11}H_{11}BrO_3$	$D_x = 1.757$ Mg m^{-3}
$M_r = 271.11$	Mo $K\alpha$ radiation, $\lambda = 0.71073$ Å
Orthorhombic, $Pna2_1$	Cell parameters from 9927 reflections
$a = 7.0928$ (5) Å	$\theta = 2.8$–$28.2°$
$b = 14.3933$ (10) Å	$\mu = 3.99$ mm^{-1}
$c = 10.0419$ (7) Å	$T = 150$ K
$V = 1025.17$ (12) Å^3	Block, colourless
$Z = 4$	$0.22 \times 0.06 \times 0.03$ mm
$F(000) = 544$	

Data collection

Bruker D8 QUEST PHOTON 3 diffractometer	13923 measured reflections
Radiation source: fine-focus sealed tube	2534 independent reflections
Graphite monochromator	2366 reflections with $I > 2\sigma(I)$
Detector resolution: 7.3910 pixels mm^{-1}	$R_{int} = 0.030$
φ and ω scans	$\theta_{max} = 28.3°$, $\theta_{min} = 2.8°$
Absorption correction: numerical (*SADABS*; Krause *et al.*, 2015)	$h = -9 \rightarrow 8$
	$k = -19 \rightarrow 19$
$T_{min} = 0.70$, $T_{max} = 0.89$	$l = -13 \rightarrow 13$

Refinement

Refinement on F^2	Hydrogen site location: inferred from neighbouring sites
Least-squares matrix: full	H-atom parameters constrained
$R[F^2 > 2\sigma(F^2)] = 0.025$	$w = 1/[\sigma^2(F_o^2) + (0.0247P)^2 + 0.097P]$ where $P = (F_o^2 + 2F_c^2)/3$
$wR(F^2) = 0.056$	
$S = 1.08$	$(\Delta/\sigma)_{max} = 0.001$
2534 reflections	$\Delta\rho_{max} = 0.41$ e Å^{-3}
139 parameters	$\Delta\rho_{min} = -0.39$ e Å^{-3}
1 restraint	Absolute structure: Flack x determined using 1025 quotients $[(I^+)-(I^-)]/[(I^+)+(I^-)]$ (Parsons *et al.*, 2013). Refined as an inversion twin
Primary atom site location: dual	
Secondary atom site location: difference Fourier map	Absolute structure parameter: 0.039 (12)

Special details

Experimental. The diffraction data were obtained from 3 sets of frames, each of width 0.50 ° in ω or φ, collected with scan parameters determined by the "strategy" routine in *APEX4*. The scan time was 10.00 sec/frame.

Geometry. All esds (except the esd in the dihedral angle between two l.s. planes) are estimated using the full covariance matrix. The cell esds are taken into account individually in the estimation of esds in distances, angles and torsion angles; correlations between esds in cell parameters are only used when they are defined by crystal symmetry. An approximate (isotropic) treatment of cell esds is used for estimating esds involving l.s. planes.

Refinement. Refinement of F^2 against ALL reflections. The weighted R-factor wR and goodness of fit S are based on F^2, conventional R-factors R are based on F, with F set to zero for negative F^2. The threshold expression of $F^2 > 2\text{sigma}(F^2)$ is used only for calculating R-factors(gt) etc. and is not relevant to the choice of reflections for refinement. R-factors based on F^2 are statistically about twice as large as those based on F, and R- factors based on ALL data will be even larger. H-atoms attached to carbon were placed in calculated positions (C—H = 0.95 - 0.99 Å). All were included as riding contributions with isotropic displacement parameters 1.2 - 1.5 times those of the attached atoms. One reflection affected by the beamstop was omitted from the final refinement. Refined as a 2-component inversion twin.

Fractional atomic coordinates and isotropic or equivalent isotropic displacement parameters (Å^2)

	x	*y*	*z*	U_{iso}*/U_{eq}
Br1	0.26616 (4)	0.95085 (2)	0.61925 (8)	0.02538 (11)
O1	0.2173 (3)	0.77072 (17)	0.7610 (2)	0.0259 (5)
O2	0.3585 (3)	0.56410 (13)	0.3929 (2)	0.0217 (5)
O3	0.4552 (3)	0.66801 (14)	0.1506 (2)	0.0265 (6)
C1	0.3410 (4)	0.81569 (19)	0.4184 (3)	0.0153 (6)
C2	0.2942 (4)	0.8293 (2)	0.5505 (3)	0.0171 (6)
C3	0.2657 (3)	0.7523 (2)	0.6327 (5)	0.0184 (7)
C4	0.2862 (4)	0.6621 (2)	0.5822 (3)	0.0191 (7)
H4	0.266176	0.610159	0.638782	0.023*
C5	0.3355 (4)	0.6484 (2)	0.4500 (3)	0.0173 (6)
C6	0.3652 (4)	0.7259 (2)	0.3673 (3)	0.0155 (6)
C7	0.4207 (4)	0.73116 (19)	0.2271 (3)	0.0172 (6)
C8	0.4287 (5)	0.8336 (2)	0.1892 (3)	0.0214 (7)
H8A	0.341666	0.846478	0.114395	0.026*
H8B	0.558028	0.850884	0.161645	0.026*
C9	0.3700 (4)	0.8891 (2)	0.3127 (3)	0.0201 (7)
H9A	0.470112	0.933291	0.339159	0.024*
H9B	0.252057	0.923961	0.296052	0.024*
C10	0.1933 (6)	0.6945 (3)	0.8509 (4)	0.0339 (9)
H10A	0.153765	0.717936	0.938144	0.051*
H10B	0.312996	0.661020	0.860085	0.051*
H10C	0.096895	0.652214	0.816037	0.051*
C11	0.3100 (5)	0.4840 (2)	0.4710 (4)	0.0248 (7)
H11A	0.320697	0.428012	0.415954	0.037*
H11B	0.180267	0.490130	0.503313	0.037*
H11C	0.396091	0.479171	0.547044	0.037*

Atomic displacement parameters (Å^2)

	U^{11}	U^{22}	U^{33}	U^{12}	U^{13}	U^{23}
Br1	0.03113 (18)	0.02045 (15)	0.02457 (17)	−0.00137 (11)	0.0002 (2)	−0.00798 (19)

O1	0.0341 (14)	0.0296 (14)	0.0140 (12)	−0.0017 (10)	0.0020 (10)	−0.0017 (10)
O2	0.0326 (13)	0.0131 (10)	0.0193 (11)	−0.0007 (9)	0.0028 (10)	0.0019 (9)
O3	0.0366 (13)	0.0231 (11)	0.0200 (14)	0.0059 (9)	0.0048 (9)	−0.0025 (9)
C1	0.0122 (14)	0.0157 (13)	0.0182 (15)	−0.0012 (12)	−0.0021 (11)	0.0019 (11)
C2	0.0160 (15)	0.0153 (14)	0.0201 (16)	0.0006 (12)	−0.0021 (12)	−0.0023 (12)
C3	0.0131 (12)	0.0277 (14)	0.014 (2)	−0.0014 (10)	−0.0025 (13)	0.0032 (17)
C4	0.0184 (15)	0.0200 (15)	0.0188 (17)	−0.0014 (12)	−0.0007 (11)	0.0039 (11)
C5	0.0145 (15)	0.0163 (14)	0.0212 (15)	0.0008 (12)	−0.0018 (12)	0.0017 (12)
C6	0.0128 (14)	0.0173 (14)	0.0163 (15)	−0.0007 (11)	0.0003 (11)	0.0010 (12)
C7	0.0160 (15)	0.0171 (14)	0.0186 (15)	0.0021 (11)	−0.0013 (12)	0.0024 (12)
C8	0.0281 (18)	0.0188 (15)	0.0174 (16)	0.0020 (13)	0.0053 (13)	0.0046 (12)
C9	0.0239 (17)	0.0156 (15)	0.0210 (15)	−0.0010 (12)	0.0022 (13)	0.0001 (12)
C10	0.045 (2)	0.039 (2)	0.0182 (19)	−0.0062 (17)	0.0017 (15)	0.0042 (16)
C11	0.0346 (19)	0.0144 (14)	0.0254 (18)	−0.0033 (14)	−0.0029 (15)	0.0046 (14)

Geometric parameters (Å, º)

Br1—C2	1.892 (3)	C6—C7	1.465 (4)
O1—C3	1.359 (6)	C7—C8	1.524 (4)
O1—C10	1.431 (4)	C8—C9	1.532 (4)
O2—C5	1.352 (3)	C8—H8A	0.9900
O2—C11	1.437 (4)	C8—H8B	0.9900
O3—C7	1.215 (3)	C9—H9A	0.9900
C1—C2	1.381 (4)	C9—H9B	0.9900
C1—C6	1.401 (4)	C10—H10A	0.9800
C1—C9	1.512 (4)	C10—H10B	0.9800
C2—C3	1.396 (5)	C10—H10C	0.9800
C3—C4	1.401 (5)	C11—H11A	0.9800
C4—C5	1.387 (4)	C11—H11B	0.9800
C4—H4	0.9500	C11—H11C	0.9800
C5—C6	1.406 (4)		
C3—O1—C10	118.6 (3)	C7—C8—H8A	110.3
C5—O2—C11	117.4 (3)	C9—C8—H8A	110.3
C2—C1—C6	120.8 (3)	C7—C8—H8B	110.3
C2—C1—C9	127.5 (3)	C9—C8—H8B	110.3
C6—C1—C9	111.8 (3)	H8A—C8—H8B	108.6
C1—C2—C3	119.4 (3)	C1—C9—C8	104.0 (2)
C1—C2—Br1	120.4 (2)	C1—C9—H9A	111.0
C3—C2—Br1	120.2 (3)	C8—C9—H9A	111.0
O1—C3—C2	116.2 (3)	C1—C9—H9B	111.0
O1—C3—C4	123.4 (3)	C8—C9—H9B	111.0
C2—C3—C4	120.4 (4)	H9A—C9—H9B	109.0
C5—C4—C3	120.3 (3)	O1—C10—H10A	109.5
C5—C4—H4	119.8	O1—C10—H10B	109.5
C3—C4—H4	119.8	H10A—C10—H10B	109.5
O2—C5—C4	124.4 (3)	O1—C10—H10C	109.5
O2—C5—C6	116.3 (3)	H10A—C10—H10C	109.5

C4—C5—C6	119.3 (3)	H10B—C10—H10C	109.5
C1—C6—C5	119.8 (3)	O2—C11—H11A	109.5
C1—C6—C7	109.7 (2)	O2—C11—H11B	109.5
C5—C6—C7	130.5 (3)	H11A—C11—H11B	109.5
O3—C7—C6	128.6 (3)	O2—C11—H11C	109.5
O3—C7—C8	124.0 (3)	H11A—C11—H11C	109.5
C6—C7—C8	107.5 (2)	H11B—C11—H11C	109.5
C7—C8—C9	107.0 (2)		
C6—C1—C2—C3	−1.8 (4)	C9—C1—C6—C5	−177.2 (3)
C9—C1—C2—C3	177.4 (3)	C2—C1—C6—C7	−177.9 (3)
C6—C1—C2—Br1	178.9 (2)	C9—C1—C6—C7	2.8 (3)
C9—C1—C2—Br1	−1.9 (4)	O2—C5—C6—C1	178.9 (3)
C10—O1—C3—C2	−177.7 (3)	C4—C5—C6—C1	−1.3 (4)
C10—O1—C3—C4	2.7 (4)	O2—C5—C6—C7	−1.0 (5)
C1—C2—C3—O1	−179.1 (3)	C4—C5—C6—C7	178.8 (3)
Br1—C2—C3—O1	0.3 (3)	C1—C6—C7—O3	179.4 (3)
C1—C2—C3—C4	0.6 (4)	C5—C6—C7—O3	−0.7 (5)
Br1—C2—C3—C4	179.9 (2)	C1—C6—C7—C8	−0.7 (3)
O1—C3—C4—C5	179.8 (3)	C5—C6—C7—C8	179.2 (3)
C2—C3—C4—C5	0.2 (4)	O3—C7—C8—C9	178.4 (3)
C11—O2—C5—C4	6.6 (5)	C6—C7—C8—C9	−1.5 (3)
C11—O2—C5—C6	−173.7 (3)	C2—C1—C9—C8	177.2 (3)
C3—C4—C5—O2	179.9 (3)	C6—C1—C9—C8	−3.6 (3)
C3—C4—C5—C6	0.2 (4)	C7—C8—C9—C1	3.0 (3)
C2—C1—C6—C5	2.1 (4)		

Hydrogen-bond geometry (Å, º)

D—H···*A*	*D*—H	H···*A*	*D*···*A*	*D*—H···*A*
C11—H11*A*···Br1[i]	0.98	3.06	3.605 (4)	116
C11—H11*C*···Br1[ii]	0.98	2.90	3.683 (3)	137
C11—H11*C*···O3[iii]	0.98	2.58	3.288 (4)	129

Symmetry codes: (i) −*x*+1/2, *y*−1/2, *z*−1/2; (ii) *x*+1/2, −*y*+3/2, *z*; (iii) −*x*+1, −*y*+1, *z*+1/2.